SVERIGES METEOROLOGISKA OCH HYDROLOGISKA INSTITUT
RHO 26

SMHI

TURBULENT MIXING AND PARTICLE DISTRIBUTION INVESTIGATIONS IN THE HIMMERFJÄRDEN 1978

By Erik Buch

Dnr 361/131

TURBULENT MIXING AND PARTICLE DISTRIBUTION INVESTIGATIONS IN THE HIMMERFJÄRD 1978

By Erik Buch

SMHI Reports

HYDROLOGY AND OCEANOGRAPHY

No RHO 26 (1980)

Undersökningar av turbulent omblandning och partikelfördelning i Himmerfjärden 1978

SVERIGES METEOROLOGISKA OCH HYDROLOGISKA INSTITUT
Norrköping 1980

ISSN 0347-7827

Page No

CONTENTS

ABSTRACT

Turbulent diffusion in the weak halocline in the Himmerfjärd in the fall was studied by a tracer experiment. The tracer, Rhodamine B, was injected instantaneously at a prescribed depth and after that the spreading of the dye patch was followed by a systematic mapping of the concentration distribution.

Vertical exchange coefficients computed from the experiment range from $1.9 \cdot 10^{-2}$ to $3.1 \cdot 10^{-2}$ cm^2/s. The vertical exchange is rather weak in comparison with results from open waters at the same windspeed and stratification. This is thought to be due to a reduction of the wind induced mixing caused by the physical boundaries of the narrow fiord.
Horizontal diffusion characteristics are computed from the time rate of change of the concentration distribution variances. Apparent horizontal diffusivities range up to about $5 \cdot 10^3$ cm^2/s when the observed scale of turbulence ranges up to about 800 m.

The results are not consistent with a model for generation of horizontal dispersion by vertical current shear and vertical diffusion and it is concluded that horizontal diffusion and also horizontal shear are important factors for generation of dispersion in the Himmerfjärd.
Particle distribution in the Himmerfjärd was investigated by measuring vertical profiles of light attenuation at a number of stations. The results show a layering of the fiord into three distinct layers such that the particle content is relatively high in the upper and the bottom layer and relatively low in the intermediate layer. The intermediate layer is believed to be intruding Baltic water.

The work has been carried out by Dr Erik Buch, Institute of Physical Oceanography, University of Copenhagen. It is a part of the project "Materialtransporter i Himmerfjärden" financed by grants to SMHI from the Research Department of the Swedish Environment Protection Board, contract nr 7-329/79. This project is intended to give hydrographic information for the system ecological study "Himmerfjärdsundersökningen" run by the Askö Laboratory. Project leader at SMHI is Erland Bergstrand. The tracer study was initiated in a cooperation between Dr Wayne Wilmot at the RGASA group, University of Stockholm and Dr Erik Buch.

TURBULENT MIXING AND PARTICLE DISTRIBUTION INVESTIGATIONS IN THE HIMMERFJÄRD 1978

INTRODUCTION

The Himmerfjärd has been thoroughly investigated physically, chemically and biologically during the last years in order to develop models describing the processes which are judged to be important for longterm balances of material.
For the modelling there is a need of information about the horizontal and vertical turbulent diffusion and the particle distribution in the Himmerfjärd, wherefore a number of dye diffusion- and optical light transmission experiments has been carried out during the week 2 - 6 October 1978 onboard the research vessel "Aurelia".

INSTRUMENTATION AND EXPERIMENTAL TECHNIQUE

1. Diffusion experiments

The turbulent diffusion has been investigated by means of a dye tracing method using the organic, fluorescent liquid Rhodamine B as a tracer. An in situ fluorometer, described by Kullenberg (1968, 1974), has been used for the tracing. Information about the current, especially the current shear, and the density stratification during the period of diffusion experiments was gained by means of a permanent current meter station and thermistor chain station measuring the current, the salinity and the temperature every two meters in the depth interval 4 - 16 meters. The dye experiments were carried out in the pycnocline layer, because it is of special interest to know the mixing between the two layers in stratified waters.

The density of the dye was adjusted to the density of the depth of injection within 0.1 σ_t - units, and the dye was injected by

means of high pressure of 4 - 10 atm through a hose connected to a two meter long diffusor. The injection lasted for about five minutes which means that the release of dye may be regarded as momentaneous after 2 - 3 hours, according to the criterion given by Okubo (1971). When the dye patch, mainly because of the current shear, was spread out horizontally a systematic mapping of the concentration distribution started.

The fluorometer, in tow at the shipside, was cycling in a depth interval around the depth of injection. During the experiments in the Himmerfjärd radar bearings were used for position determinations.
The duration of the experiment was 12 - 16 hours. Observations of the wind were made at intervals during the whole experiment.

2. Particle distribution investigations

For determination of the particle distribution a light attenuation meter (c - meter) was used. The path length of the c - meter is 1.4 m and it measures the light attenuation coefficient $\underline{c}$ in the red (λ_{max} = 655 nm), the green (λ_{max} = 525 nm) and the ultraviolet (λ_{max} = 380 nm) part of the spectrum. However, in the Himmerfjärd the content of material, especially yellow substance, was so great that all utraviolet light was totally attenuated along the 1.4 m long path.
Vertical profiles were made at 11 stations placed in such a way that longitudinal and transversal sections of particle distribution were obtained, see Fig 1.

RESULTS

Symbols used are listed on page 15.

1. Vertical diffusion

Assuming that

a) the advective terms may be disregarded because the observations are made in a Lagrangian reference system with origo at the center of the dye patch,

b) the vertical velocity is negligible,

c) the decrease in the dye concentration is due only to vertical diffusion, and

d) the vertical diffusion coefficient K is a constant, the general diffusion equation is reduced to

1) $$\frac{\partial C}{\partial t} = K \cdot \frac{\partial^2 C}{\partial z^2}$$

Because radar navigation was used in the Himmerfjärd, the observations were made in an absolute reference system, but during the data processing they were transformed into a Lagrangian system by considering the drift velocities, so that the assumption a) still holds.

A solution to eq 1 has been given by Kullenberg (1968):

2) $$K = \frac{H^2}{\pi^2 (t_2 - t_1)} \ln \frac{C_1}{C_2}$$

where subscripts 1 and 2 denote successive times of observation. Identification of a given layer with increasing diffusion time has been done by means of thickness, shape and position in the temperature structure.

The mixing coefficients obtained by the experiments in the Himmerfjärd are given in Table 2.

Kullenberg (1971; 1974) found theoretically the relation

3) $$K = Rf\ c_d \frac{\rho_a}{\rho_o} \left(\frac{W_a}{N}\right)^2 \left|\frac{dq}{dz}\right|$$

by assuming that

a) the turbulence is shear generated, and

b) the internal stress is approximately equal to the surface wind stress.

The coefficient of proportionality ($Rf\ c_d \frac{\rho_a}{\rho_o}$) can be found from the observations by plotting K versus $\left(\frac{W_a}{N}\right)^2 \left|\frac{dq}{dz}\right|$

From investigations in open sea- and coastal areas, Kullenberg found:

4) $$Rf\ c_d \frac{\rho_a}{\rho_o} = 9.6 \cdot 10^{-8}$$

for persisting winds ($W_a \geq 4\text{-}5$ m/s).

In Fig 17 the results from the present investigations in the Himmerfjärd are given together with results obtained by the author in areas similar to the Himmerfjärd, Buch (1978, 1979). It is seen that the coefficient

5) $$Rf\ c_d \frac{\rho_a}{\rho_o} = 1.3 \cdot 10^{-9}$$

is considerably smaller than the value obtained by Kullenberg. Mixing experiments giving this low vertical mixing have all been carried out in narrow fiords and so it is believed that the physical boundaries are reducing the mixing effect due to the wind.

In Table 4 is given an evaluation of the entrainment from the lower to the upper layer. The entrainment velocity, u_e, is here calculated as

$$u_e = \frac{KN^2}{g'}$$ (Kullenberg 1977)

In a theory of Kato and Phillips (1969) for entrainment due to shear generated turbulence there is given the relation

$$u_e / u_* = 2.5\ Ri_*^{-1}$$

In Table 4 the quantities of this relation are calculated whereby the friction velocity u_* is assumed to be given by the wind only. The reduced wind fetch mentioned above will here have the effect that the constant of proportionality between u_e / u_* and Ri_*^{-1} is very much lower than the one obtained by Kato and Phillips (1969).

2. Horizontal diffusion

A mean picture of the horizontal dye concentration distribution has been obtained by plotting the observed concentrations along the track of the ship and contouring the plot. To get a picture as accurate as possible the dye patch must be covered in a number of directions but, on the other hand, the time used for one proper covering of the patch must not exceed more than about 20% of the diffusion time.

Examples of concentration distribution pictures obtained in the Himmerfjärd are shown in Figs 7 - 16.

To get information about the horizontal diffusion characteristics from the dye distribution the theory of Joseph and Sendner (1958) can be used. The observed distribution of the dye has been transformed into a rotationally symmetric one by calculating the equivalent radius r, i.e. the radius of a circle with an area equivalent to the area inside a given concentration isoline.

The theory gives an equation for calculation of the horizontal diffusion velocity P:

6) $$\sigma_{rc}^2 = 6\ P^2\ t^2$$

where

7) $$\sigma_{rc}^2 = \frac{\int_o^\infty r^2 C(r,t) 2\pi r dr}{\int_o^\infty C(r,t) 2\pi r dr}$$

is the definition of the rotationally symmetric variances, see Table 5.

As seen in Figs 7 - 16 the distribution of dye is not rotationally symmetric, but is more like an ellipse. Therefore it may be more accurate to find the longitudinal and transversal variances

σ_x^2 and σ_y^2

defined by

8) $$\sigma_x^2 = \frac{\int\int_{-\infty}^{+\infty} x^2 C dxdy}{\int\int_{-\infty}^{+\infty} C dxdy}$$

9) $$\sigma_y^2 = \frac{\int\int_{-\infty}^{+\infty} y^2 C dxdy}{\int\int_{-\infty}^{+\infty} C dxdy}$$

The vertical distribution is assumed homogenous.

If the dye distribution is Gaussian, the definition of σ_{rc}^2 writes

10) $$\sigma_{rc}^2 = \sigma_x \sigma_y$$

In Table 6 a comparison of σ_{rc}^2 and $\sigma_x \sigma_y$ is given. As expected, there is some scattering in the results, owing partly to experimental uncertainties and partly to the fact that the dye distribution is neither rotationally symmetric nor elliptic.

The rotationally symmetric variance σ_{rc}^2 is also used for definition of the apparent horizontal diffusivity.

11) $$K_h = \frac{\sigma_{rc}^2}{4t}$$

and the scale of turbulence

12) $$l_h = 3\sigma_{rc}$$

By plotting σ^2_{rc} versus the time t and K_h versus l_h the following relations are found

13) $$\sigma^2_{rc} \sim t^{2.2}$$

14) $$K_h \sim l_h^{4/3}$$

As seen from Figs 18 and 19 the present results are very similar to the results of Kullenberg (1974), which means that the dye patch has spread out horizontally in a way that could be foreseen. $\sigma^2_{rc} \sim t^{2.2}$ would by using eq 11) and 12) give $K_h \sim l^{1.1}$. This inconsistency with the observed result may be due to the uncertainties in determining σ_{rc}.
In many areas it is found that the horizontal dispersion is determined by the vertical diffusion and the vertical current shear, and often to such a degree that the horizontal diffusion may be neglected, as exemplified by the findings of Kullenberg (1968).

15) $$P = (1.1\ H_o \frac{dq}{dz} + 1.3) \times 10^{-2}$$

By considering the shear - diffusion effect in an internal unbounded layer and by neglecting the vertical convection, the horizontal diffusion and the horizontal shear, Kullenberg (1971, 1974) developed a model which describes the apparent horizontal dispersion generated by the vertical diffusion and the vertical current shear.
In case of an instantaneous cubic source of dye with an initial thickness H_o, the model leads to a prediction of the horizontal variances:

16) $$\sigma^2_x = (2/3\ a_o^2\ t^3 + \frac{a^2}{\omega^2} t)\ K + \frac{1}{12}\ a_o^2\ H_o^2\ t^2$$

17) $$\sigma_y^2 = \left(9/8 \frac{b^2}{\omega^2} t + \frac{b^2 a}{a^2 \omega^2} (2 a_o - a) \right) K$$

The results obtained using this model are given in Table 7. Comparing the theoretical horizontal variances with those obtained from the experiments given in Table 6, it appears that the theoretical values are much lower than the observed ones. This implies that some of the assumptions made in developing the model do not hold in the Himmerfjärd and similar areas, Buch (1978, 1979). If the apparent diffusion velocity P is calculated fom eq. 15, see Table 7, values about an order of magnitude lower than the observed ones is found, which indicates that the horizontal diffusion may not be neglected. The horizontal shear is also expected to be important in narrow areas like the Himmerfjärd.

3. Particle distribution

The attenuation cofficient c at the wavelength λ and the depth z consists of three components:

18) $$c(\lambda, z) = c_p(\lambda, z) + a_y(\lambda, z) + c_w(\lambda)$$

The attenuation due to dissolved organic matter (yellow substance) is very wavelength selective with high attenuation in the ultraviolet and almost no attenuation in the green and red part of the spectrum. This has been utilized for an in situ determination of a_y, Jerlov (1976):

19) $$a_y(380) = \left(c(380) - c_w(380) \right) - K \left(c(655) - c_w(655) \right)$$

where K is a factor dependent upon the particle characteristics. As mentioned above, the content of yellow substance in the Himmerfjärd was so great that the ultraviolet light was totally attenuated, which means that $a_y(380)$ can not be determined.

However, the wavelength selectivity of yellow substance leads to:

20) $$c(\lambda, z) = c_p(\lambda, z) + c_w(\lambda)$$

for $$\lambda = \begin{cases} 525 \text{ nm} \\ 655 \text{ nm} \end{cases}$$

According to Clarke and James (1939), the attenuation coeffients for pure water are:

$$c_w(525) = 0.041 \text{ m}^{-1}; \qquad c_w(655) = 0.304 \text{ m}^{-1}$$

Optical measurements were carried out three times during the period 2 - 6 October 1978.
From linear regression analysis the following relationship has been obtained:

21) $$c(525) = 1.24\ c(655) - 0.34$$

On this background only longitudinal and transversal sections showing the attenuation coefficient in the red due to particles are represented in this report, see Figs 20 - 25.
The observations show that the water in the Himmerfjärd can be divided into three distinct layers, a homogeneous upper layer with a relatively high content of particles, an intermediate layer of clear water, and a bottom layer rich on particles.

The behaviour of the three layers during the week of observations indicates an intrusion of clear and warm Baltic water (see Figs 2 - 6, 20 - 21) in the depth interval 6 - 12 meters during the days before 2 October. In the following days this water was mixed up with water from the other two layers, making the intermediate layer less distinct.
The observations from the 6 October indicate a new intrusion of Baltic water.
Unfortunately, the current meters between 6 - 10 meters were out of order during the whole period of observations, but the current meter at 12 meter showed in-going currents in the days up to the

2 October and again at the 6 October.
The upper layer had a rather homogeneous distribution of particles probably due to wind generated turbulent mixing.
The thickness of the upper layer was about 6 meters at the 2 October increasing to about 10 - 12 meters at the 6 October.

The increase in thickness of the upper layer can not be used directly for an estimation of the vertical diffusion coefficient, because the particle content is not a conservative property (waste water discharge, biological activity etc.) and sedimentation of particles from the upper to the intermediate layer may also be of some inportance. In connection to the light attenuation measurements Secchi disc observations were carried out too, and a Secchi disc depth of 3.8 meters was found at all the optical stations.
A Secchi disc depth of 3.8 meters means that the depth of the euphotic zone, defined as the depth at which 1% of the surface quanta irradiance is found, lies in the depth interval 6.5 - 8 meters, Højerslev (1978).
According to Jerlows (1976) optical classification, the Himmerfjärd then belongs to coastal water type no. 9.

CONCLUSIONS

The mixing experiments carried out in the Himmerfjärd October 1978 have shown that in such a narrow area the physical boundaries affect the mixing characteristics.
A dependence of the vertical mixing on the stratification, the current shear and the wind has been proved, but the constant of proportionality is much lower than the one found in open areas.
The horizontal dispersion progressed in a manner that could be expected from the diffusion diagrams given in Figs 18 - 19, but a prediction of the dispersion using Kullenbergs advection - diffusion model has indicated that horizontal diffusion and

especially horizontal shear are of importance in the Himmerfjärd. On this background it would be advisable in future experiments to investigate the horizontal shear.
The optical observations have shown a layering of the Himmerfjärd waters with three distinct layers, where the intermediate layer is believed to be intruding Baltic Water.

ACKNOWLEDGEMENTS

The author is grateful to Erland Bergstrand, Wayne Wilmot and Ulf Larsson for the practical arrangement of the experiments. Warm thanks are also given to the participants in the cruise and the crew onboard "Aurelia".
Financial support has been received from the Swedish Natural Science Council.

LIST OF SYMBOLS

a, b	oscillating vertical current shear
a_o	mean vertical current shear
a_y	light attenuation coefficient due to dissolved organic substance
c_d	drag coefficient
C	concentration, mass per unit volume
c	light attenuation coefficient
c_p	light attenuation coefficient due to particle
c_w	light attenuation coefficient due to pure water
g	acceleration of gravity
g'	reduced gravity
H_o	initial thickness of the dye layer
2h, H	thickness of the dye layer
h_1	depth to interfacial layer
K	vertical turbulent transport coefficient for mass
K_x, K_y	turbulent transport coefficients in the x, y directions, respectively
M_o	mass of injected dye
N	Brunt-Väisälä frequency
P	horizontal diffusion velocity
q	horizontal current vector
r	equivalent radius
Rf	flux Richardson number
Ri	Richardson number
$Ri_* =$	$\frac{g' \cdot h_1}{u_*^2}$; overall Richardson number
S	salinity
T	temperature
t	time
u,v,w	velocities in the x, y, z directions, respectively
U,V	mean horizontal velocities
u',v',w'	fluctuating velocities
u_*	friction velocity
u_e	entrainment velocity
W_a	wind velocity
x,y,z	Cartesian coordinate system
ε	dissipation of turbulent energy per unit mass and time
ρ	density
ρ_a	density of the air
τ	stress
τ_o	wind stress at the sea surface
ω	frequency of an oscillating current
σ_t	$= (\rho_{S,T,0}-1)\ 10^3$
σ_x^2 σ_y^2	variances of the concentration distribution in the x, y directions
σ_{rc}^2	horizontal symmetrical variance

REFERENCES

Batchelor, G K (1950): The application of the similarity theory of turbulence to atmospheric diffusion. Q.J1.R. Met. Soc., 76.

Buch, E (1978): Mixing processes in estuarine systems, especially the Belts and Norwegian fiords. Inst Phys Ocean, U of Copenhagen, rep no 38.

Buch, E (1979): Mixing experiments in fiords. Fjord Oceanographic Workshop, Canada. June 1979.

Clarke, G L and James, H R (1939): Laboratory analysis of the selective absorption of light in sea water, J Opt Soc Am, 29.

Højerslev, N (1978): Daylight measurements appropriate for photosynthetic studies in natural sea waters. J Cons int Explor Mer 38(2): 131-146.

Jerlov, N G (1976): Marine optics. Elsevier, Amsterdam, 2nd ed. 203pp.

Joseph, J and H Sendner (1958): Über die horizontale Diffusion im Meere. Deutche Hydrogr Z 11(2), 49-77.

Kato, H and O M Phillips (1969): On the penetration of a turbulent layer into a stratified fluid. J Fluid Mech 37(4), 643-655.

Kullenberg, G (1968): Measurements of horizontal and vertical diffusion in coastal waters. Inst Phys Ocean, U of Copenhagen, rep no 3.

Kullenberg, G (1971): Results of diffusion experiments in the upper layer of the sea. Inst Phys Ocean, U of Copenhagen, rep nr 12.

Kullenberg, G (1974): An experimental and theoretical investigation of turbulente diffusion in the upper layer of the sea. Inst Phys Ocean, U of Copenhagen, rep no 25.

Kullenberg, G (1976a): Note on entrainment in natual stratified vertical shear flows. Paper no 3 from the 10th Conference of Baltic Oceanographers, June 1976.

Kullenberg, G (1976): Interim report on mixing studies. Beltproject, Danish Enviromental Protection Agency.

Kullenberg, G (1977): Entrainment velocity in natural vertical stratified flow. Estuarine and Coastal Marine Science, 5,pp 329-338.

Okubo, A (1971): Oceanic diffusion diagrams. Deep.Sea-Res. 18(8), 789.802.

Table 1. Environmental observations: Mean stability parameter N^2, Vertical shear, local Richardson number and wind W_a.

Date	Depth interval m	N^2 sec^{-2}	$\frac{dq}{dz}$ sec^{-2}	Ri	Wind $m \cdot sec^{-1}$
781002	12.5-15	$7.8 \cdot 10^{-4}$	$6.8 \cdot 10^{-3}$	16.8	7 - 8
781003	12.5-15	$8.2 \cdot 10^{-4}$	$1.5 \cdot 10^{-2}$	3.6	7 - 10
781005	12.5-15	$5.3 \cdot 10^{-4}$	$1.3 \cdot 10^{-2}$	3.1	6

Table 2. Thickness 2h, timeinterval $t_2 - t_1$, concentration ratio C_1/C_2, mean depth, Vertical exchange coefficient K and mean K.

Date	2h cm	$t_2 - t_1$ sec	C_1/C_2	mean depth	K $cm^2\ sec^{-1}$	mean K $cm^2\ sec^{-1}$
781002	37	$2.7 \cdot 10^3$	2.00	12	$3.4 \cdot 10^{-2}$	
	36	$4.2 \cdot 10^3$	2.16	12	$2.4 \cdot 10^{-2}$	
	24	$1.6 \cdot 10^4$	22.09	12	$1.1 \cdot 10^{-2}$	$2.3 \cdot 10^{-2}$
781002	21	$1.1 \cdot 10^3$	4.20	12	$5.9 \cdot 10^{-2}$	
	20	$1.3 \cdot 10^4$	6.33	12	$6.5 \cdot 10^{-3}$	
	19	$3.5 \cdot 10^4$	20.00	12	$2.3 \cdot 10^{-3}$	$1.9 \cdot 10^{-2}$
781005	63	$1.5 \cdot 10^4$	4.06	12	$3.7 \cdot 10^{-2}$	
	68	$1.8 \cdot 10^4$	7.68	12	$4.8 \cdot 10^{-2}$	
	32	$1.5 \cdot 10^4$	6.37	12	$2.7 \cdot 10^{-2}$	
	32	$3.2 \cdot 10^3$	1.41	12	$1.2 \cdot 10^{-2}$	$3.1 \cdot 10^{-2}$

Table 3. Mean exchange coefficient $\overline{K}$, stability parameter $\overline{N^2}$, Shear $\overline{\frac{dq}{dz}}$, square of the mean wind $\overline{W_a^2}$ and the parameter $\overline{\frac{W^2}{N^2}\frac{dq}{dz}}$

Date	$\overline{K}$ $cm^2\ sec^{-1}$	$\overline{N^2}$ sec^{-2}	$\overline{\frac{dq}{dz}}$ sec^{-1}	$\overline{W_a^2}$ $cm^2\ sec^{-2}$	$\overline{\frac{W_a^2}{N^2}\frac{dq}{dz}}$ $cm^2\ sec^{-1}$
781002	$2.3 \cdot 10^{-2}$	$7.8 \cdot 10^{-4}$	$6.8 \cdot 10^{-3}$	$5.6 \cdot 10^5$	$4.9 \cdot 10^6$
781003	$1.9 \cdot 10^{-2}$	$8.2 \cdot 10^{-4}$	$1.5 \cdot 10^{-2}$	$6.1 \cdot 10^5$	$1.2 \cdot 10^7$
781005	$3.1 \cdot 10^{-2}$	$5.3 \cdot 10^{-4}$	$1.3 \cdot 10^{-2}$	$3.6 \cdot 10^5$	$8.8 \cdot 10^6$

Table 4. Mean vertical exchange coefficient $\overline{K}$, Stability parameter $\overline{N^2}$, reduced gravitational force, entrainment velocity, mean depth, square of the wind, overall Richardson number Ri_* and the ratio u_e/u_*.

Date	$\overline{K}$ $cm^2\ sec^{-1}$	$\overline{N^2}$ sec^{-1}	$g\frac{\Delta\rho}{\rho}$ $cm\ sec^{-2}$	u_e $cm\ sec^{-1}$	h_1 m	$\overline{W_a^2}$ $cm^2\ sec^{-2}$	Ri_*	u_e/u_*
781002	$2.3 \cdot 10^{-2}$	$7.8 \cdot 10^{-4}$	0.49	$3.7 \cdot 10^{-5}$	10	$5.6 \cdot 10^5$	$6.1 \cdot 10^2$	$4.1 \cdot 10^{-5}$
781003	$1.9 \cdot 10^{-2}$	$8.2 \cdot 10^{-4}$	0.59	$7.3 \cdot 10^{-6}$	13.5	$6.1 \cdot 10^5$	$6.1 \cdot 10^5$	$7.8 \cdot 10^{-6}$
781005	$3.1 \cdot 10^{-2}$	$5.3 \cdot 10^{-4}$	0.42	$3.9 \cdot 10^{-5}$	12.5	$3.6 \cdot 10^5$	$1.0 \cdot 10^3$	$5.4 \cdot 10^{-5}$

Table 5. Diffusion time, symmetrical variance σ^2_{rc}, Diffusion velocity P, apparent horizontal diffusion coefficient K_h and the horizontal lenghtscale l_h

Date	t sec	σ^2_{rc} cm^2	P cm sec^{-1}	K_h cm^2 sec^{-1}	l_h cm
781002	$3.6\cdot10^4$	$2.1\cdot10^8$	0.16	$1.5\cdot10^3$	$4.3\cdot10^4$
781003	$2.2\cdot10^4$	$3.1\cdot10^8$	0.33	$3.5\cdot10^3$	$5.3\cdot10^4$
	$2.7\cdot10^4$	$4.5\cdot10^8$	0.32	$4.2\cdot10^3$	$6.4\cdot10^4$
	$4.1\cdot10^4$	$6.3\cdot10^8$	0.25	$3.8\cdot10^3$	$7.5\cdot10^4$
781005	$2.4\cdot10^4$	$1.7\cdot10^8$	0.23	$1.8\cdot10^3$	$3.9\cdot10^4$
	$3.5\cdot10^4$	$2.1\cdot10^8$	0.17	$1.5\cdot10^3$	$4.3\cdot10^4$
	$4.6\cdot10^4$	$5.2\cdot10^8$	0.21	$2.8\cdot10^3$	$6.8\cdot10^4$

Table 6. Observed horizontal variances

Date	t sec	σ^2_x cm^2	σ^2_y cm^2	σ_y/σ_x	σ^2_{rc} cm^2	$\sigma_x\,\sigma_y$ cm^2
781002	$3.6\cdot10^4$	$5.5\cdot10^8$	$4.7\cdot10^6$	0.27	$2.1\cdot10^8$	$1.5\cdot10^8$
781003	$2.7\cdot10^4$	$1.5\cdot10^9$	$1.3\cdot10^7$	0.29	$4.5\cdot10^8$	$4.4\cdot10^8$
	$4.1\cdot10^4$	$2.3\cdot10^9$	$3.4\cdot10^7$	0.38	$6.3\cdot10^8$	$9.0\cdot10^8$
781005	$3.5\cdot10^4$	$6.3\cdot10^8$	$2.2\cdot10^8$	0.59	$2.1\cdot10^8$	$3.7\cdot10^8$
	$4.6\cdot10^4$	$4.5\cdot10^9$	$1.3\cdot10^8$	0.17	$5.2\cdot10^8$	$7.7\cdot10^8$

Table 7. Parameters for prediction of variances and predicted variances

Date	t sec	H_o cm	P (eq. 15)	K cm^2 sec^{-1}	a_o sec^{-1}	a sec^{-1}
781002	$3.6\cdot10^4$	200	0.03	$2.3\cdot10^{-2}$	$4.9\cdot10^{-3}$	$1.25\cdot10^{-3}$
781003	$4.1\cdot10^4$	200	0.05	$1.9\cdot10^{-2}$	$6.15\cdot10^{-3}$	$8.75\cdot10^{-3}$
781005	$3.5\cdot10^4$	200	0.04	$3.1\cdot10^{-3}$	$3.25\cdot10^{-3}$	$3.00\cdot10^{-3}$

Date	b sec^{-1}	ω sec^{-1}	$\sigma^2_{x_2}$ cm^2	$\sigma^2_{y_2}$ cm^2	$\sigma_{x_2}\sigma_y$ cm^2	σ_y/σ_x
781002	$9.7\cdot10^{-3}$	$4.4\cdot10^{-4}$	$1.2\cdot10^8$	$1.0\cdot10^7$	$3.5\cdot10^7$	0.29
781003	$3.3\cdot10^{-3}$	$4.4\cdot10^{-4}$	$2.5\cdot10^8$	$1.8\cdot10^5$	$6.7\cdot10^6$	0.03
781005	$2.5\cdot10^{-3}$	$4.4\cdot10^{-4}$	$4.9\cdot10^7$	$8.5\cdot10^4$	$2.0\cdot10^6$	0.04

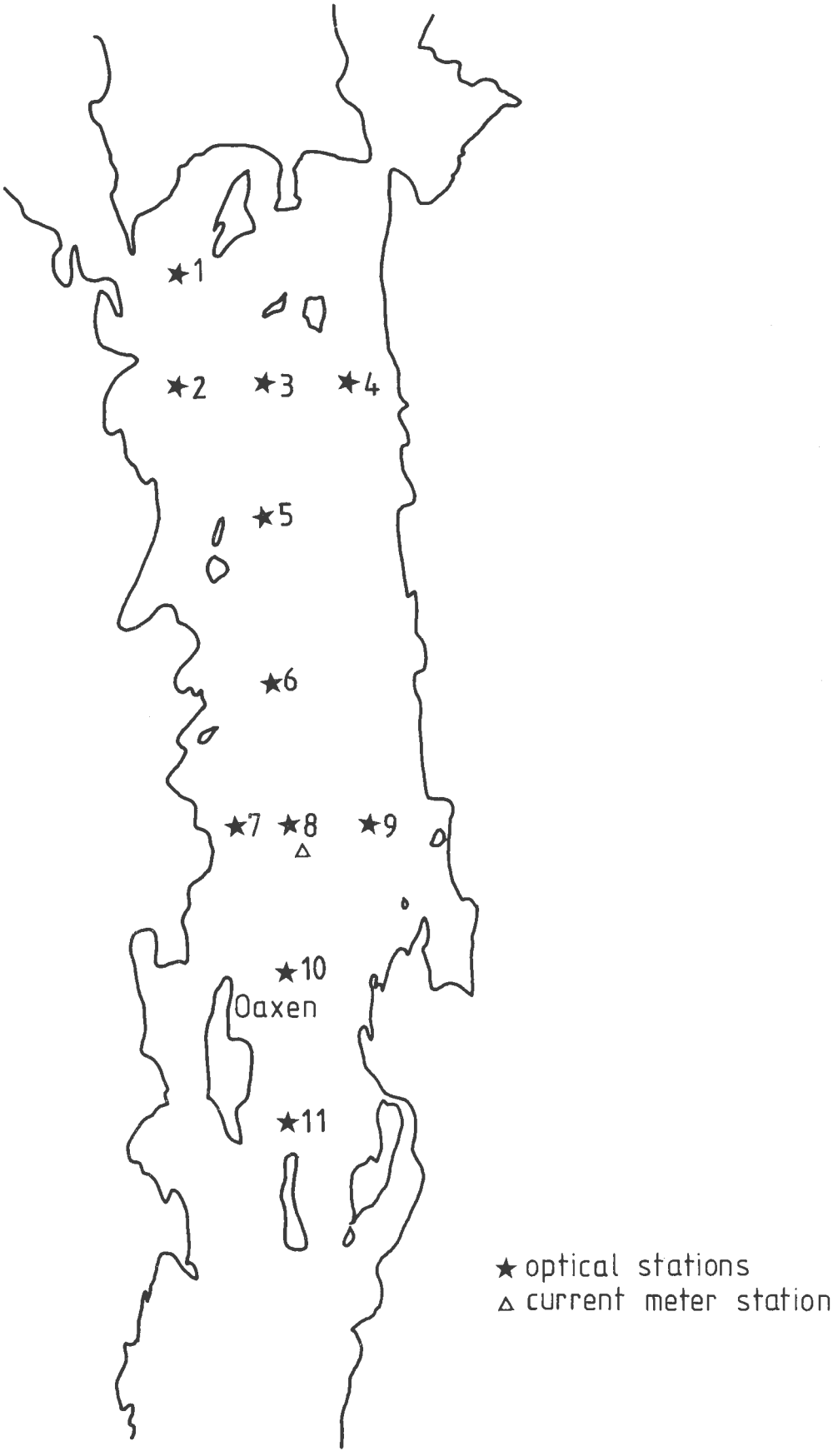

Figure 1. Area of investigation, the Himmerfjärd

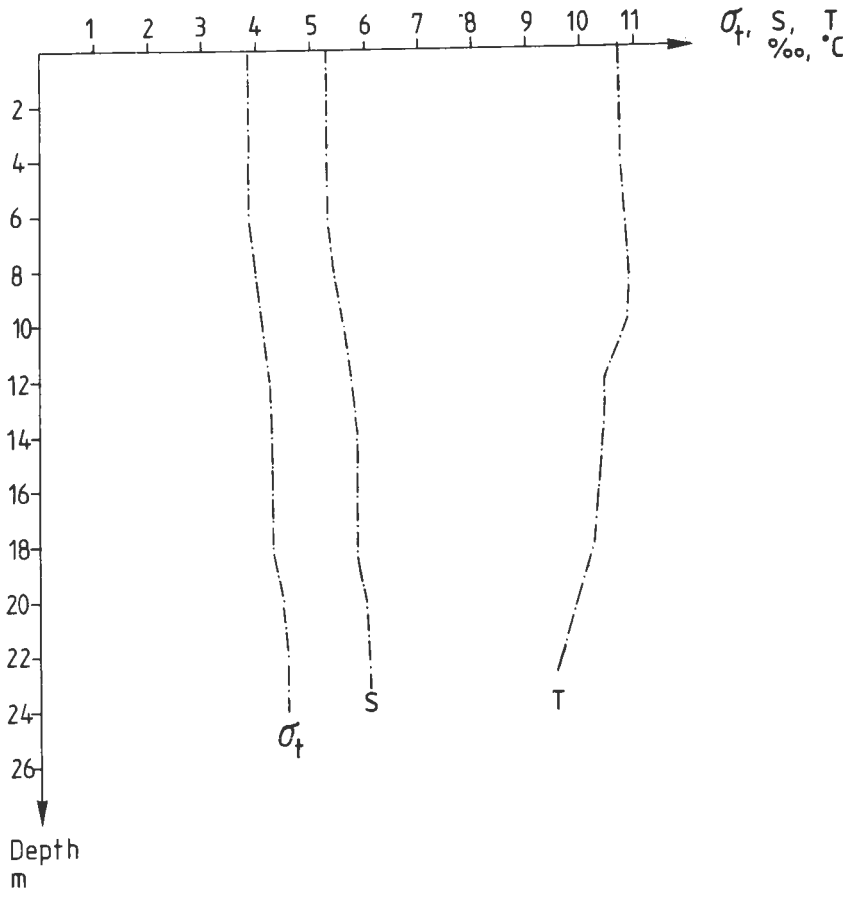

Figure 2. Vertical distribution of salinity (S), temperature (T) and density (σ_t) 781002 time 17.45

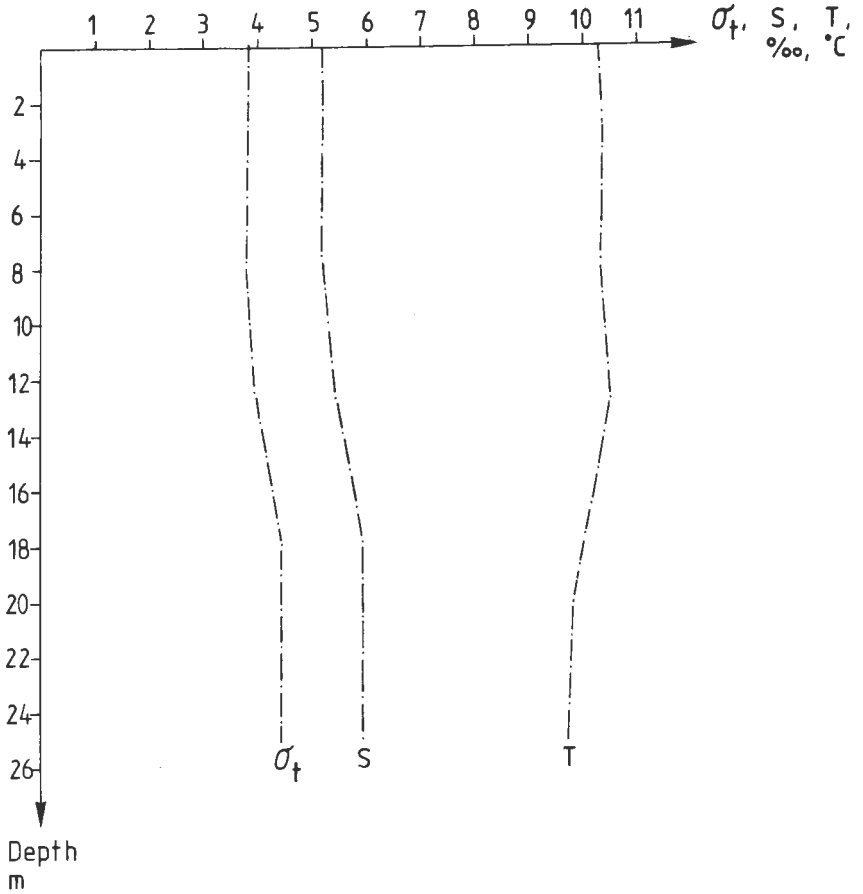

Figure 3. Vertical distribution of salinity (S), temperature (T) and density (σ_t) 781003 time 15.00

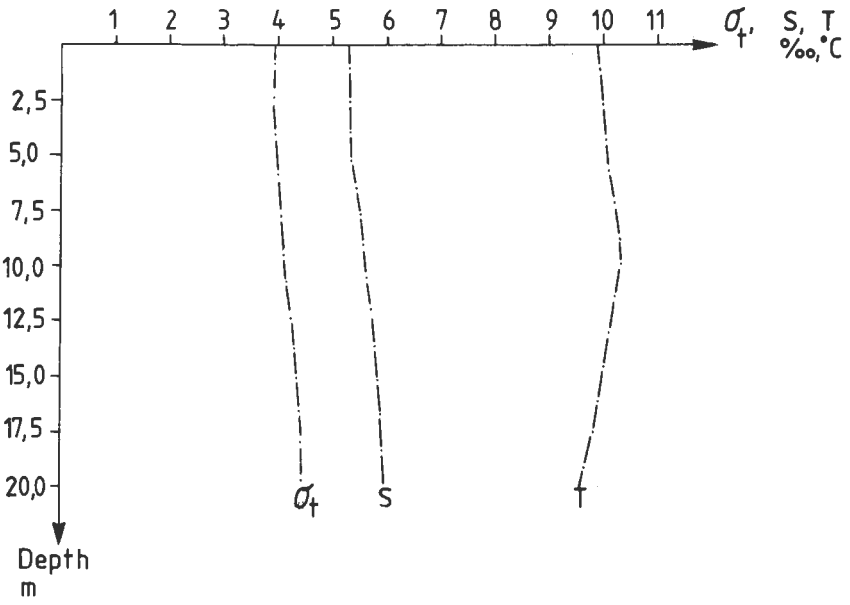

Figure 4. Vertical distibution of salinity (S), temperature (T) and density (σ_t) 781005 time 6.00

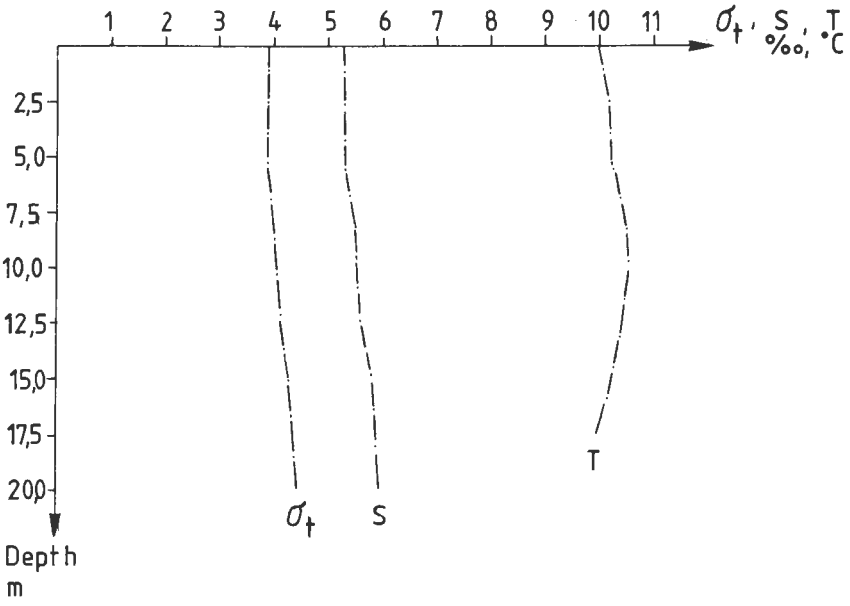

Figure 5. Vertical distribution of salinity (S), temperature (T) and density (σ_t) 781005 time 8.15

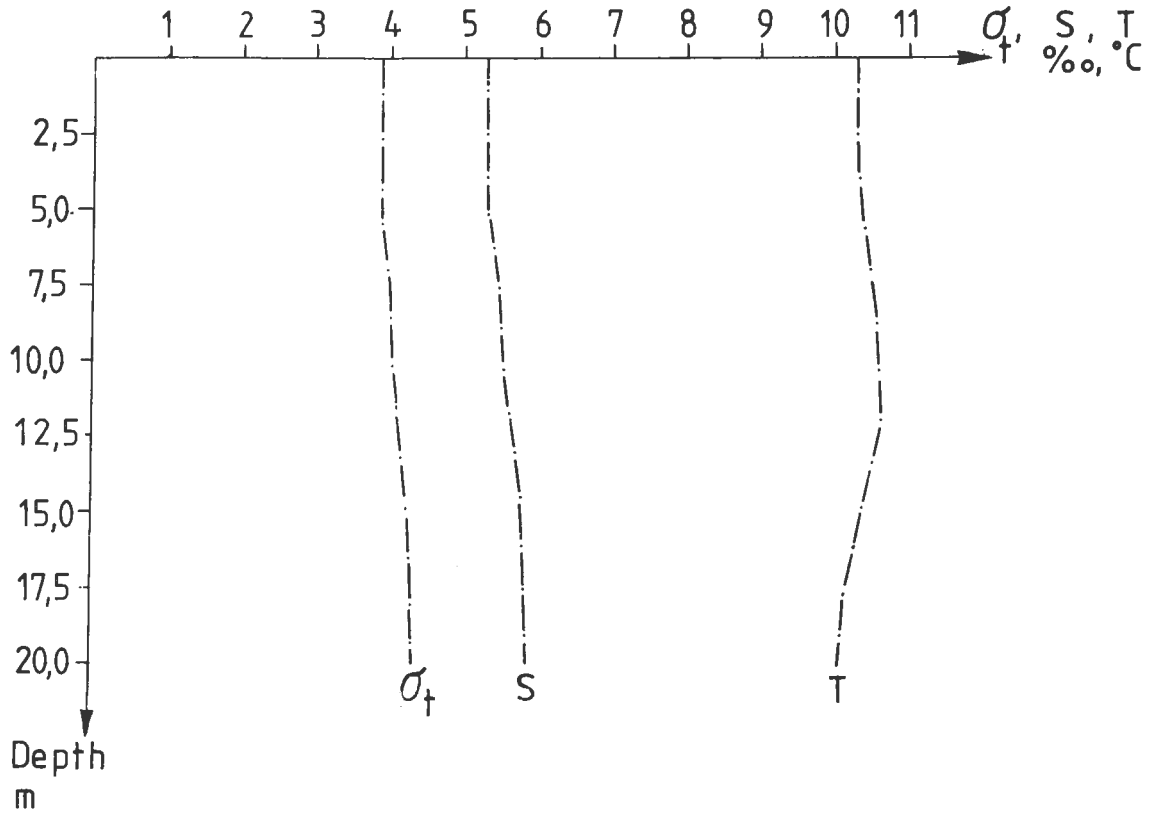

Figure 6. Vertical distribution of salinity (S), temperature (T) and density (σ_t) 781005 time 8.30

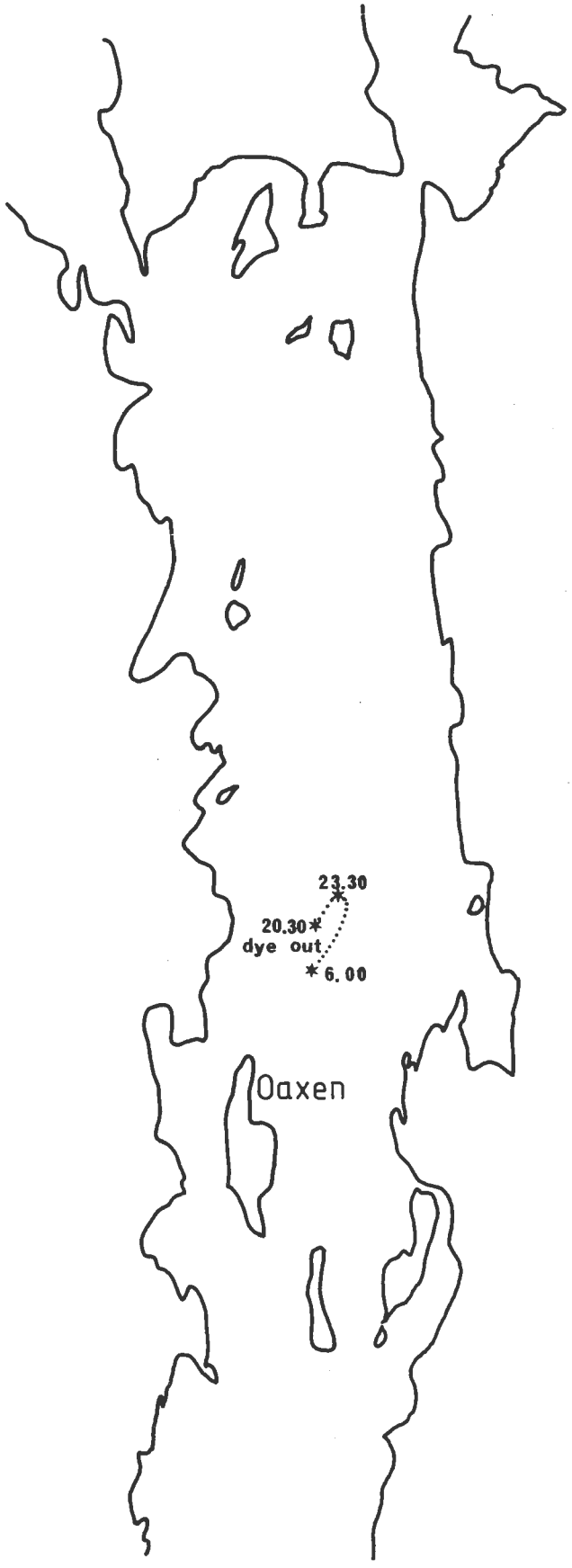

Figure 7. Track of the dye patch during experiment 1

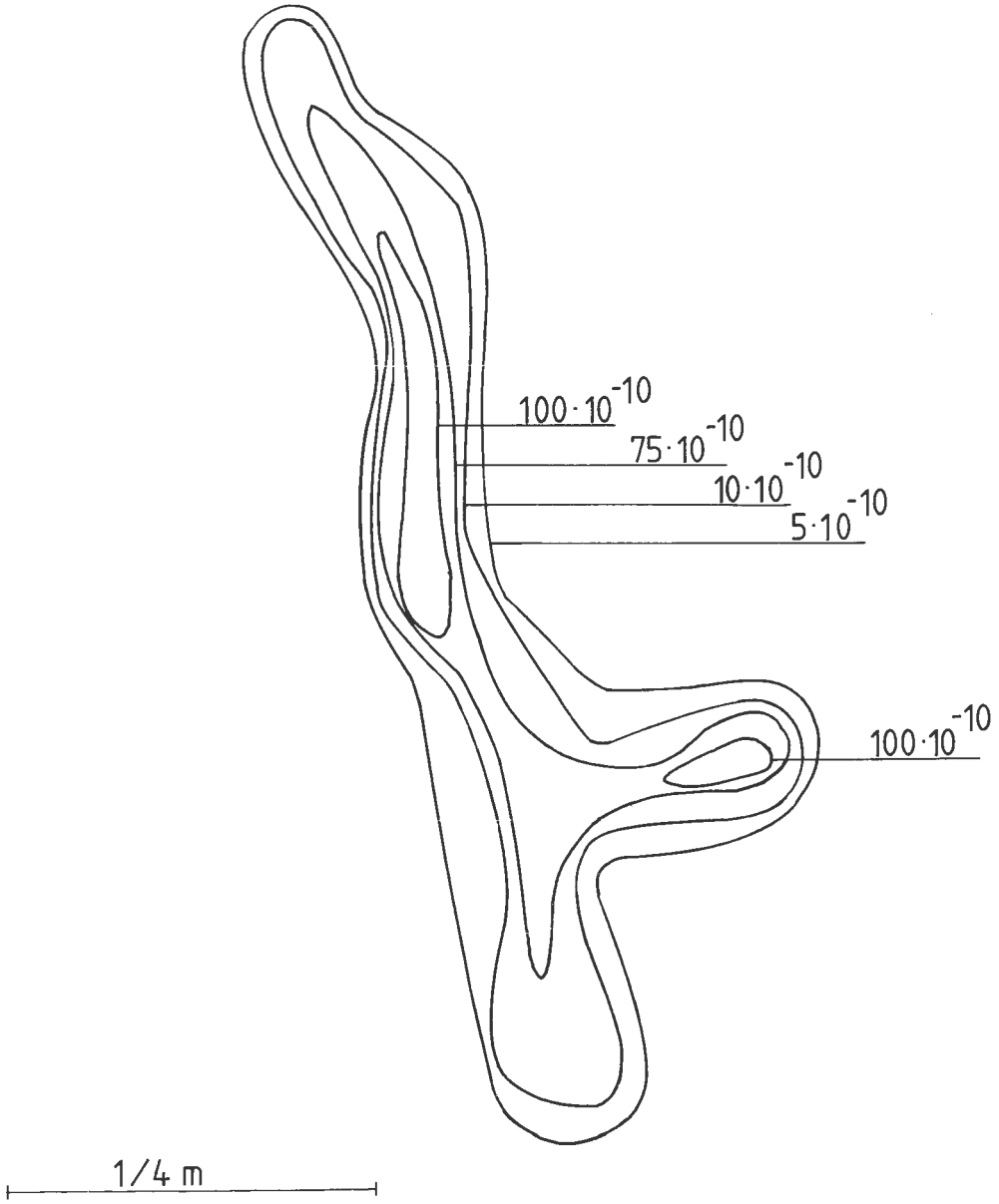

Figure 8. Dye distribution (t/m^3). 781003 time 5.06-7.23.
Experiment 1

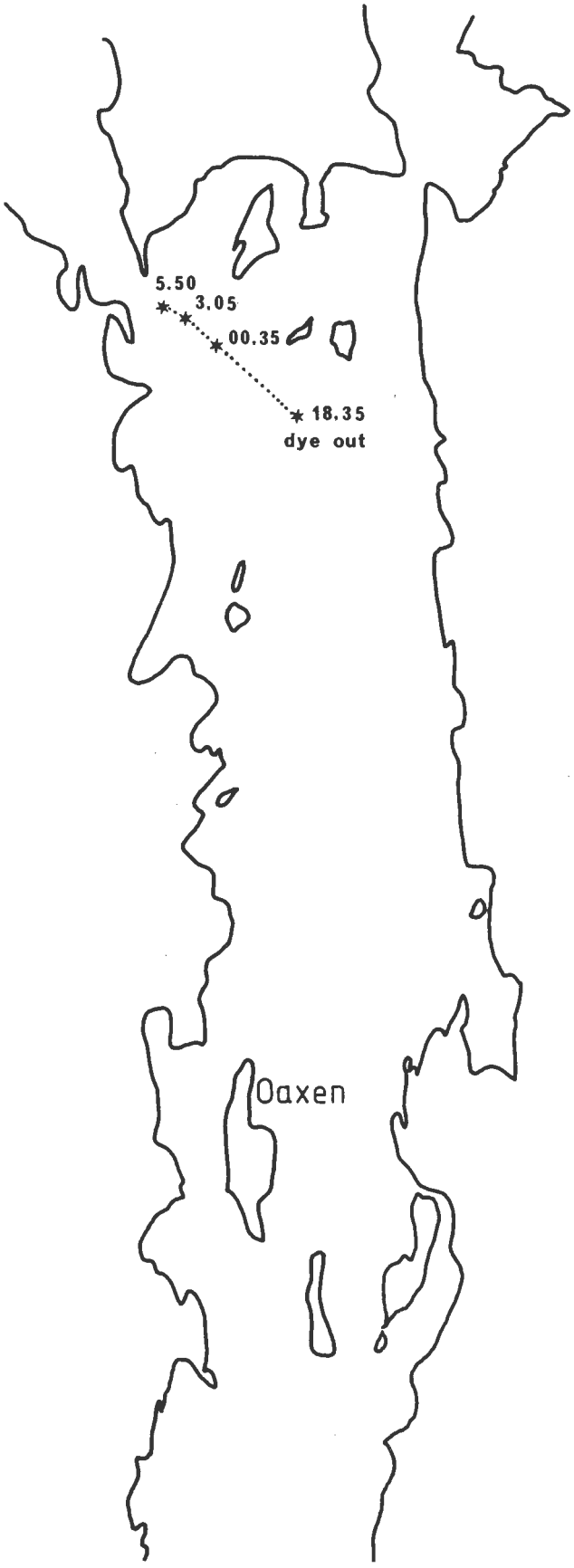

Figure 9. Track of the dye patch during experiment 2

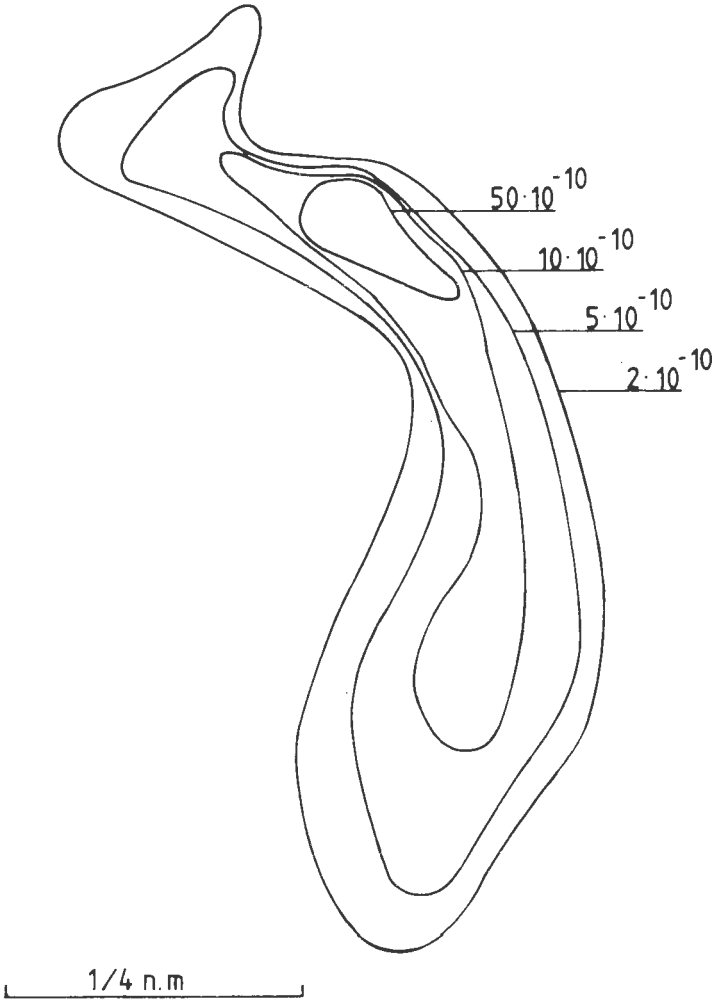

Figure 10. Dye distribution (t/m^3). 781003 time 23.22-01.53. Experiment 2

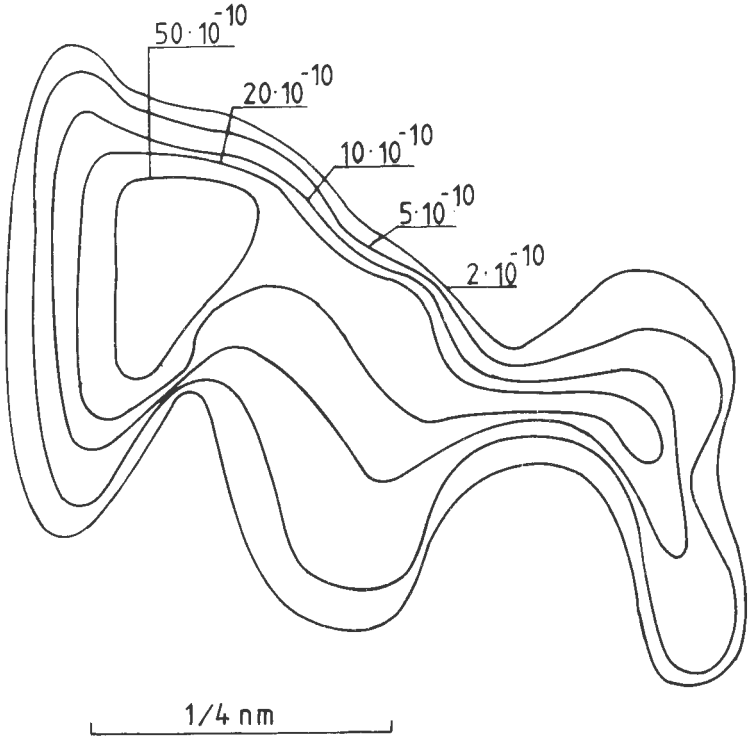

Figure 11. Dye distribution (t/m^3). 781004 time 02.22-03.56 Experiment 2

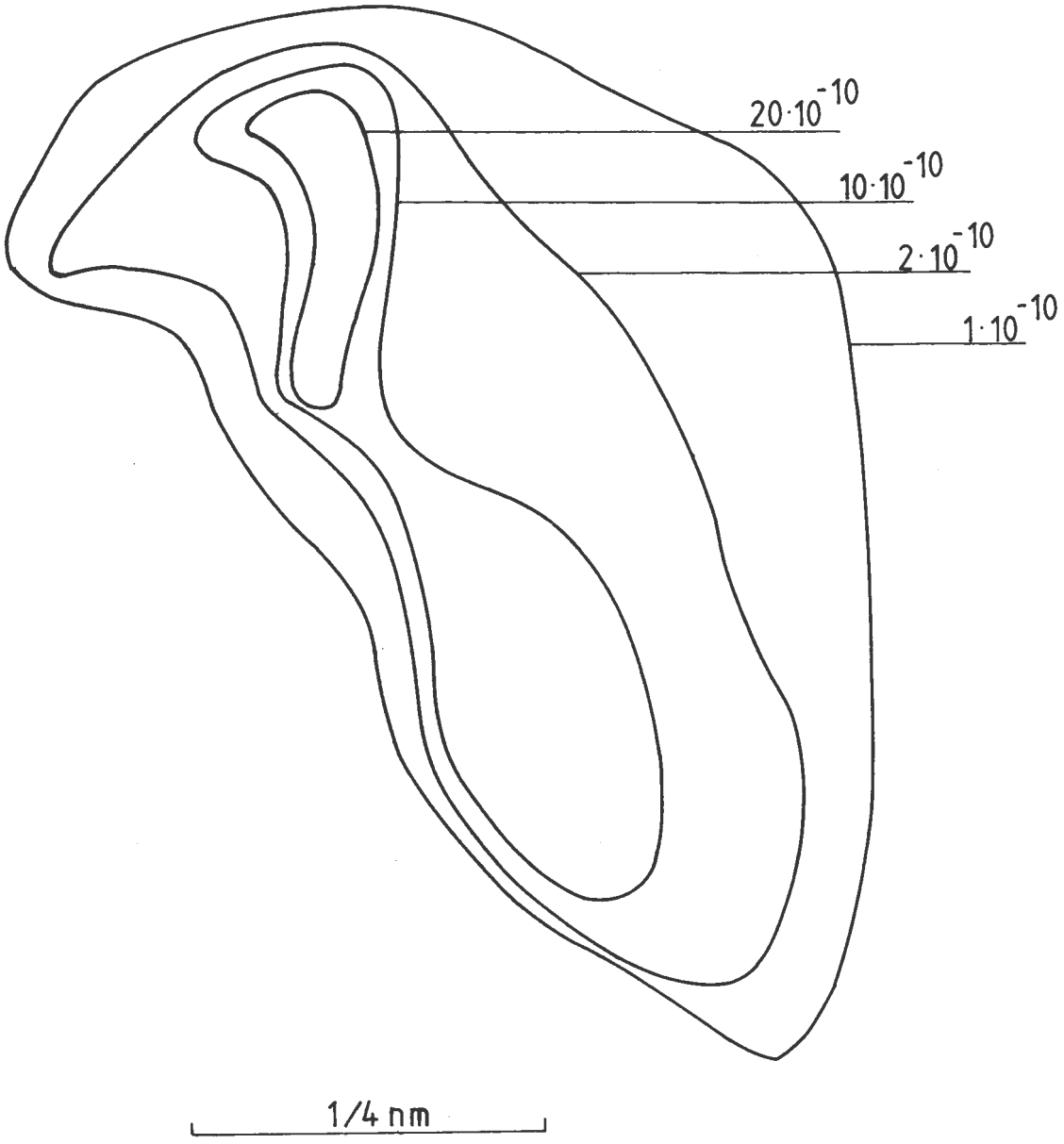

Figure 12. Dye distribution (t/m^3). 781004 time 04.57-06.59. Experiment 2

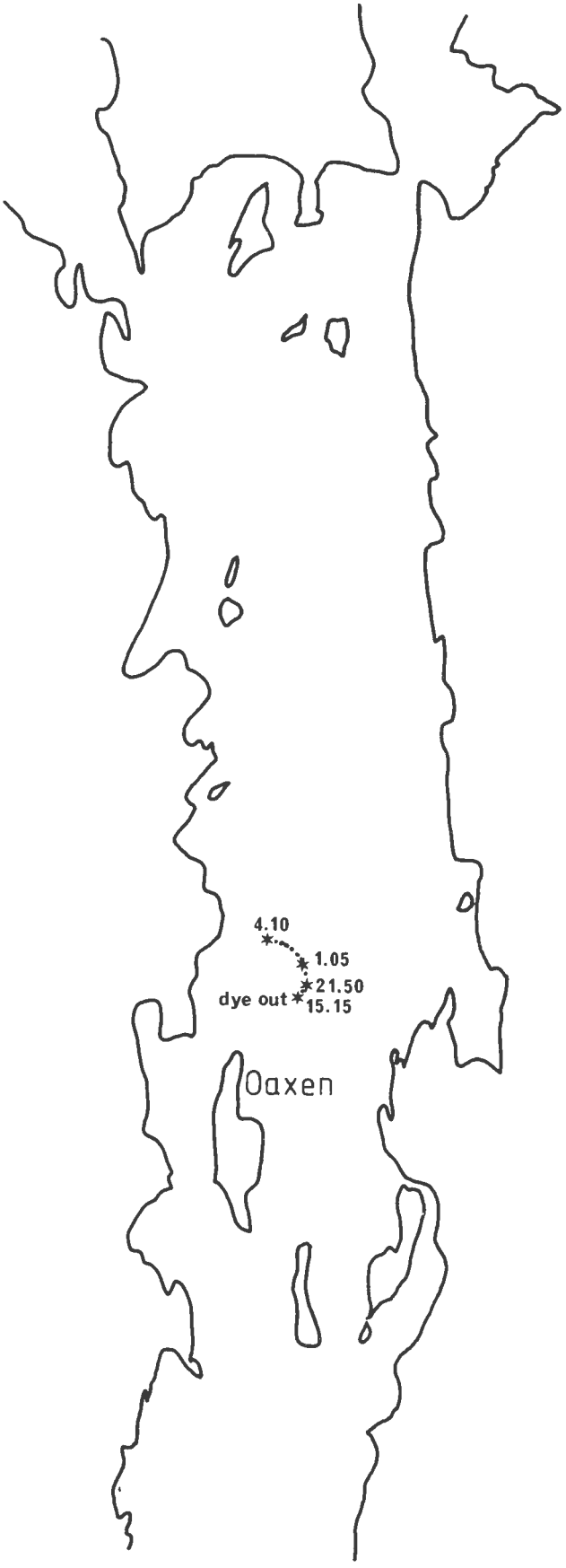

Figure 13. Track of the dye patch during experiment 3

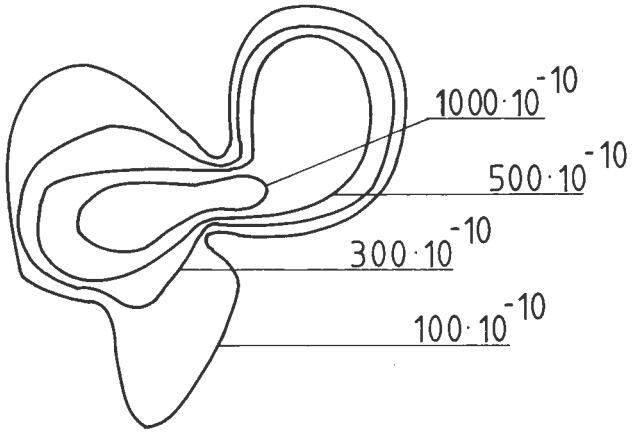

Figure 14. Dye distribution (t/m^3). 781005 time 21.13-22.36. Experiment 3

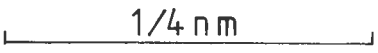

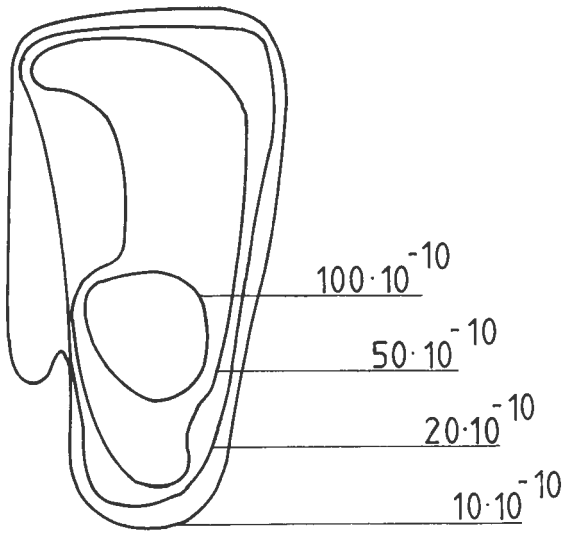

Figure 15. Dye distribution (t/m^3). 781006 time 00.33-01.41. Experiment 3

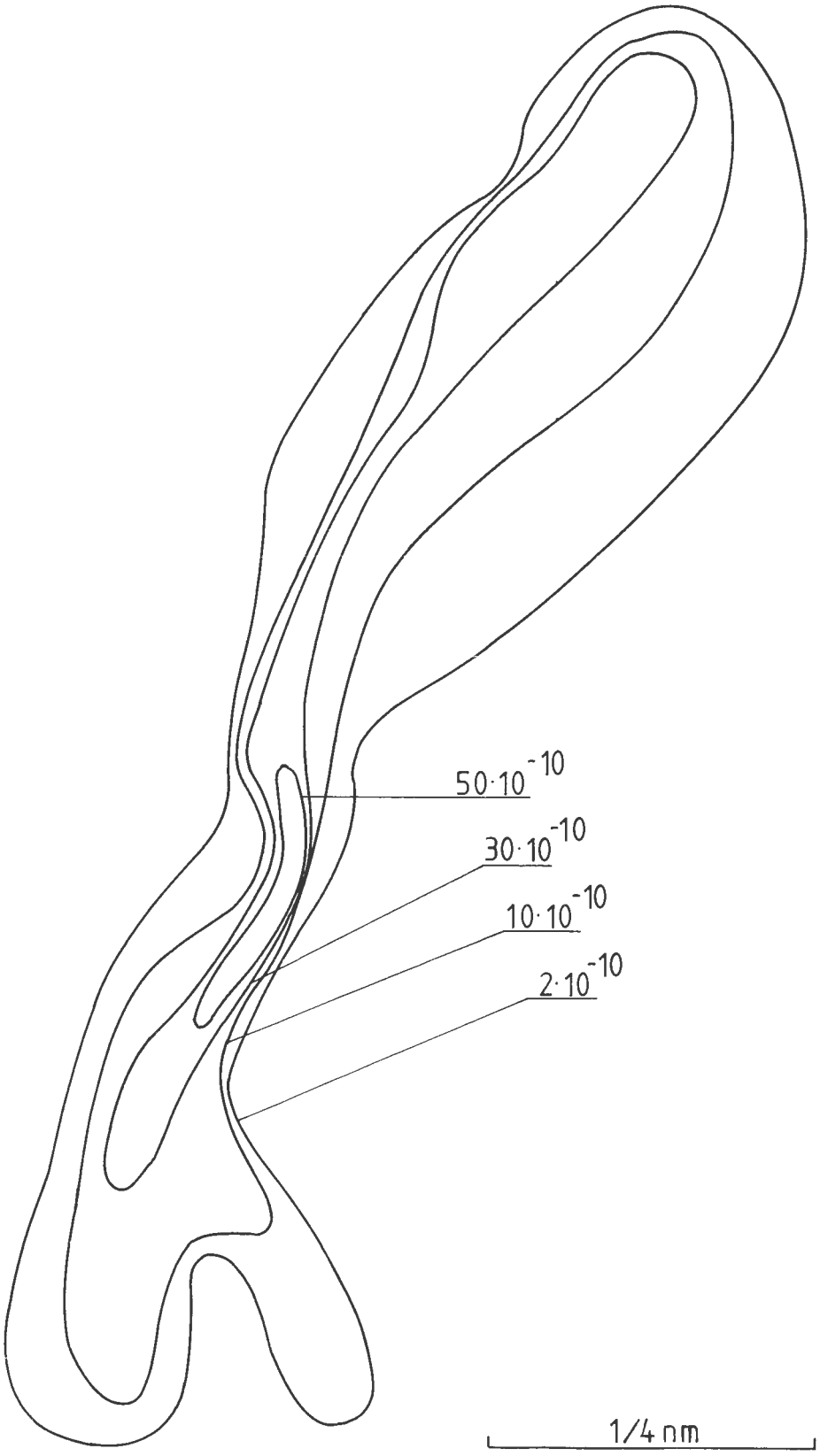

Figure 16. Dye distribution (t/m^3). 781006 time 03.03-05.16. Experiment 3

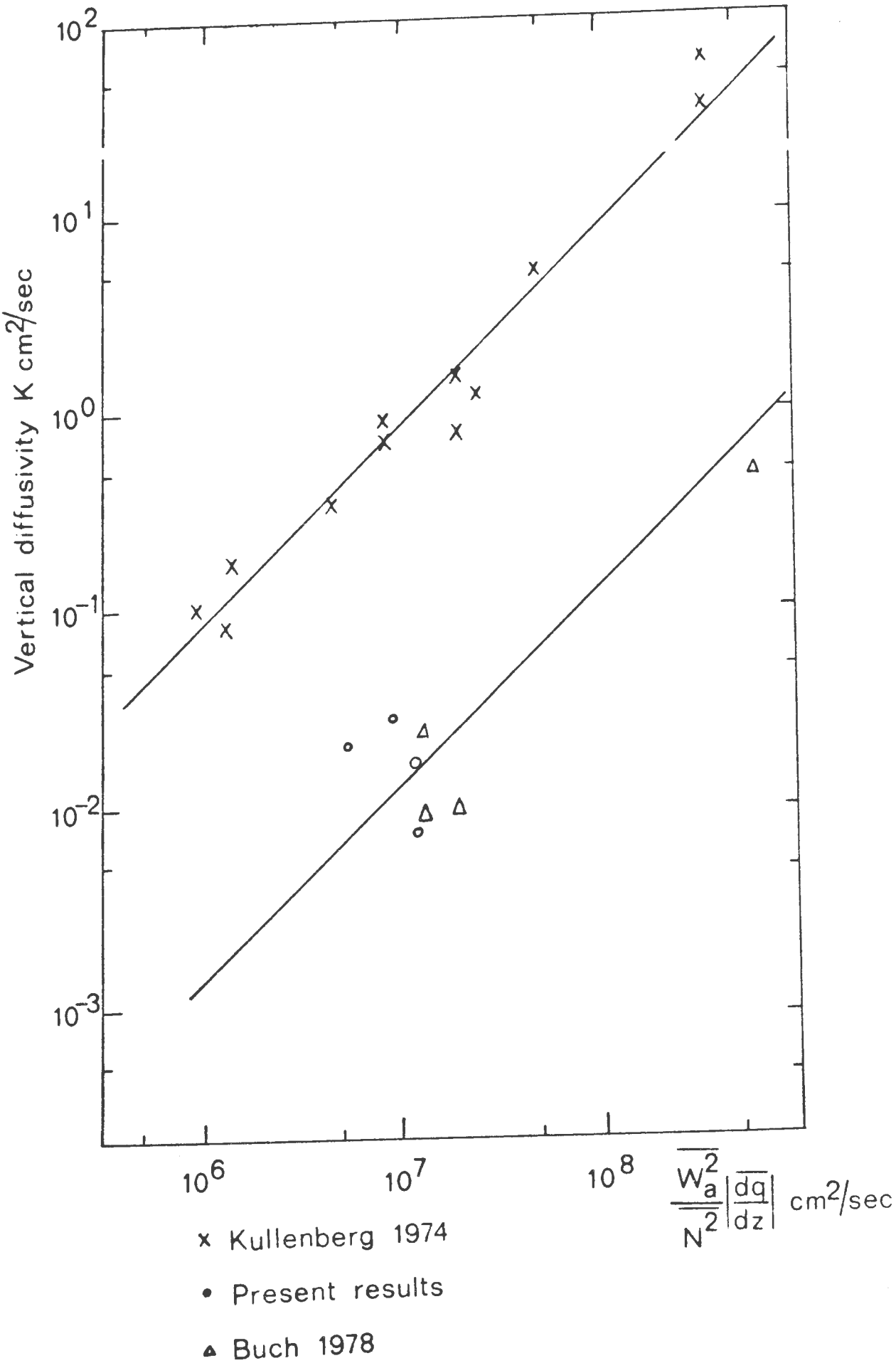

Figure 17. Vertical diffusion coefficient K versus the factor $\frac{\overline{Wa^2}}{\overline{N^2}}\left|\frac{\overline{dq}}{dz}\right|$

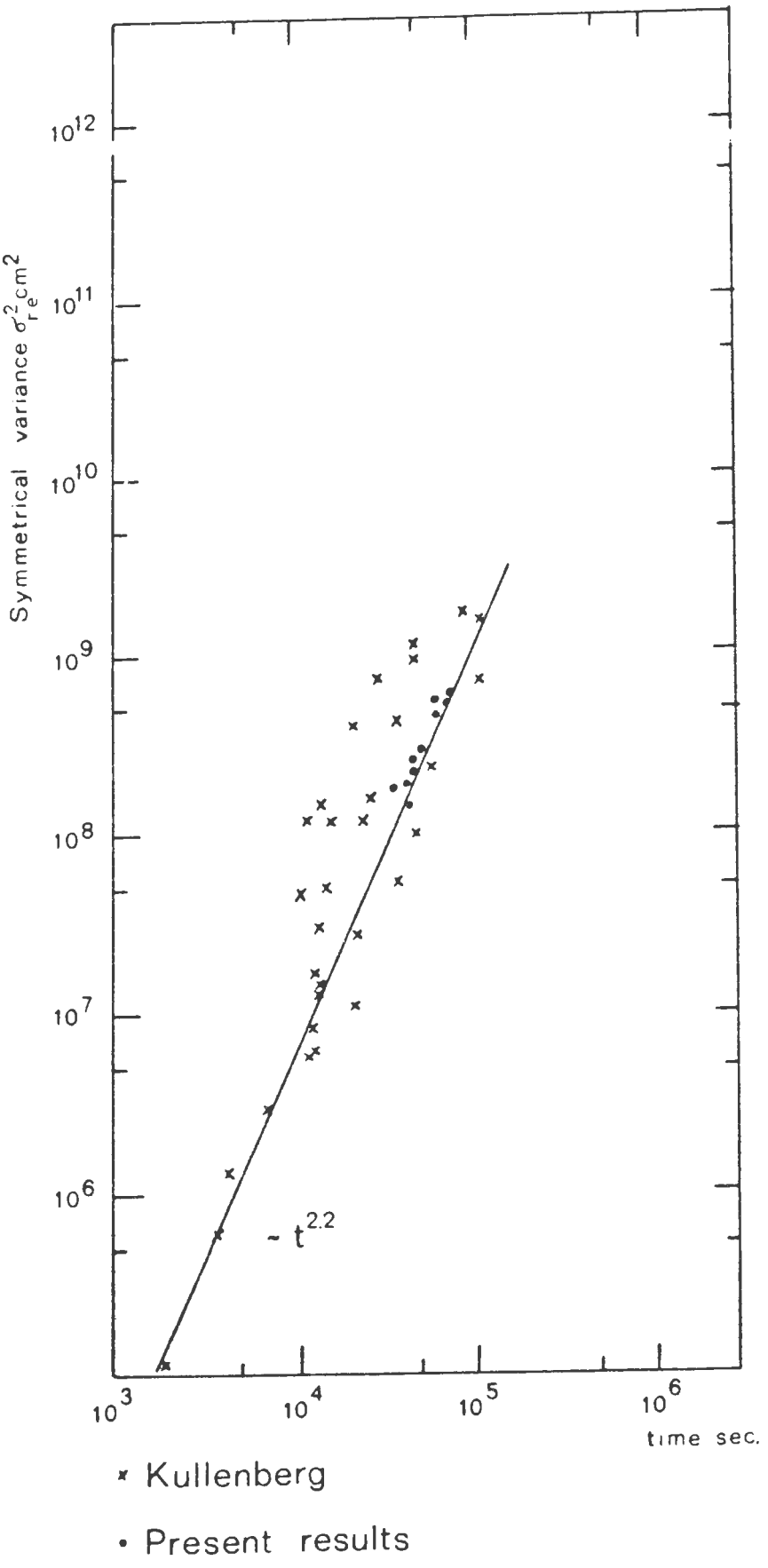

Figure 18. Symmetrical variance σ^2_{rc} versus t

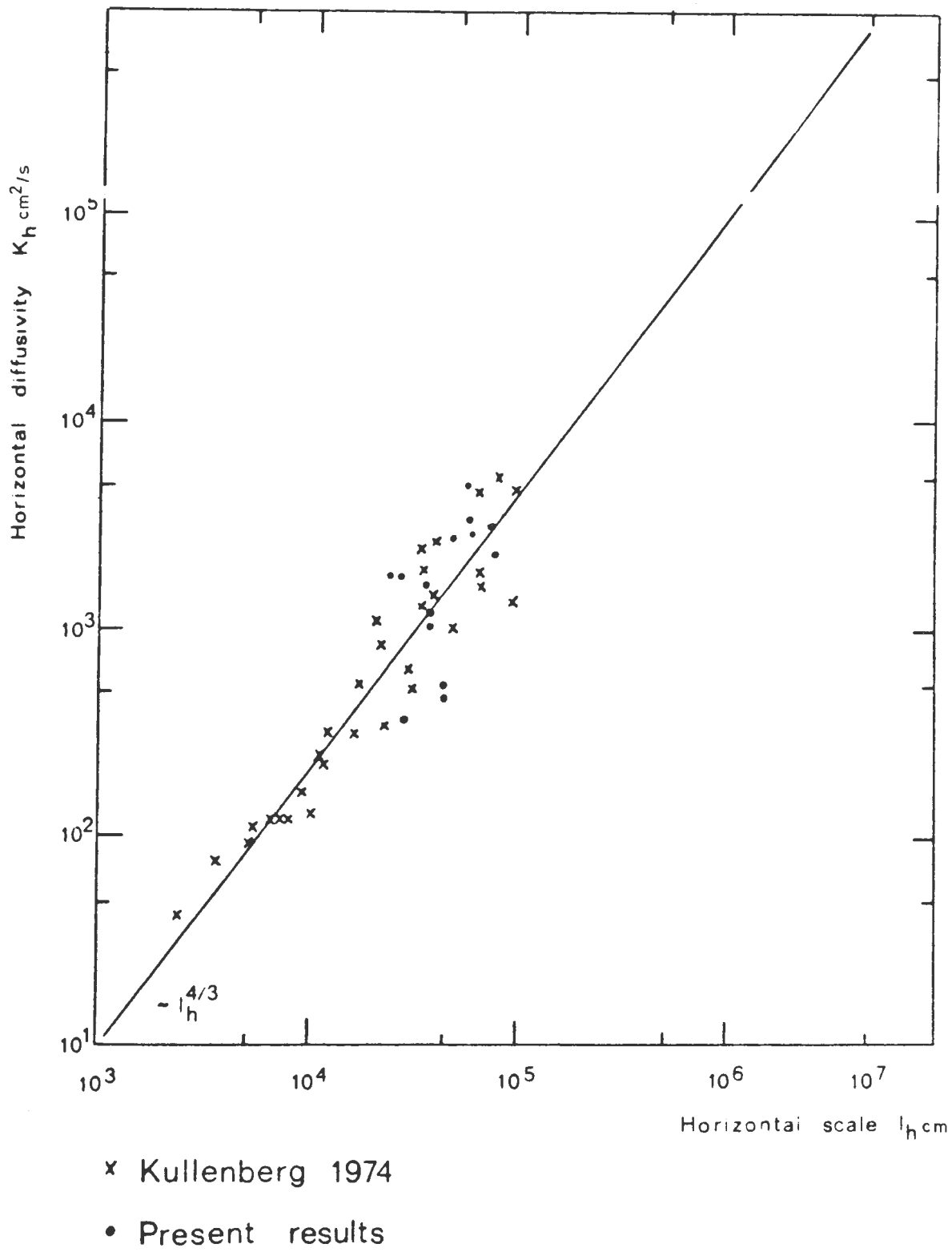

Figure 19. Horizontal diffusion coefficient K_h versus horizontal length scale l_h

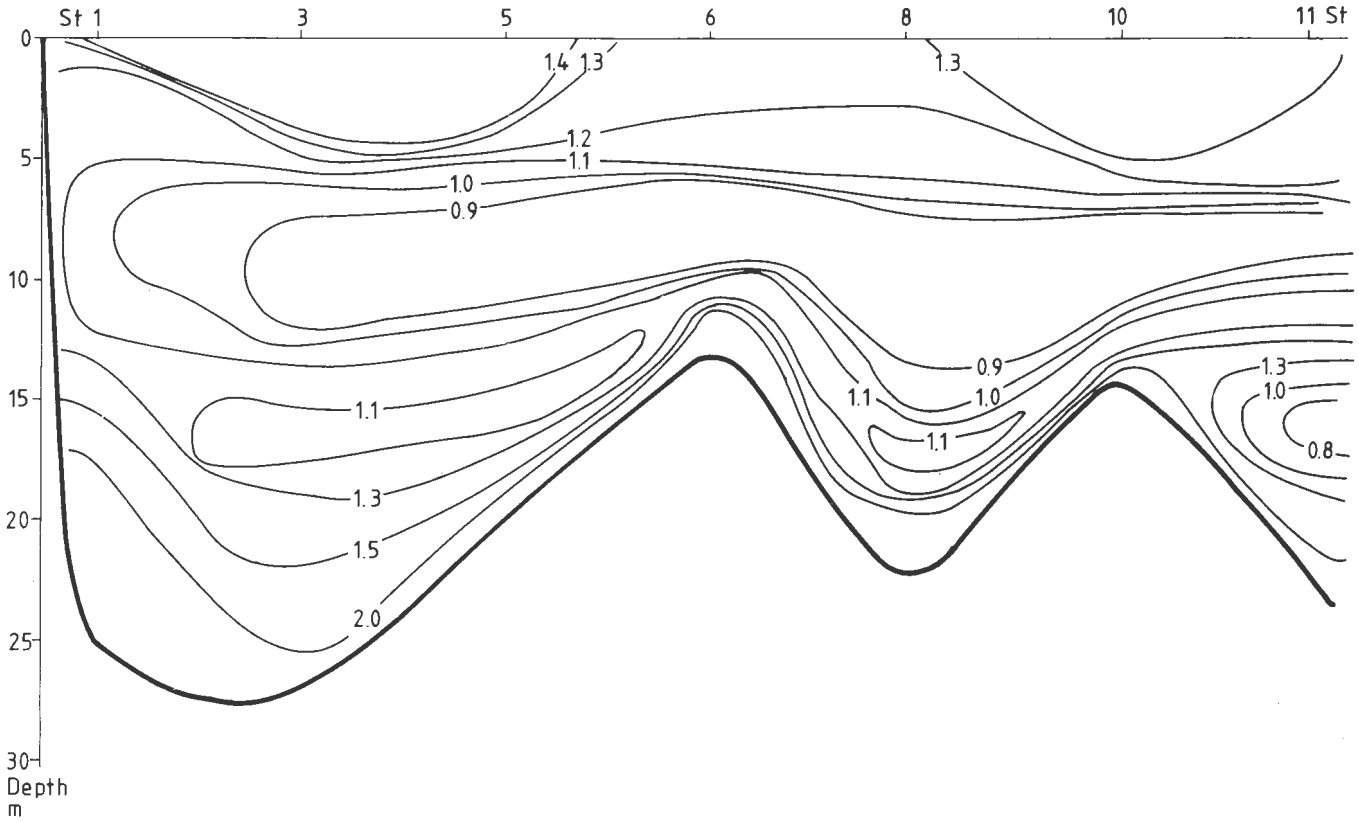

Figure 20. Distribution of c_p, attenuation coefficient due to particles. Longitudinal section. 781002

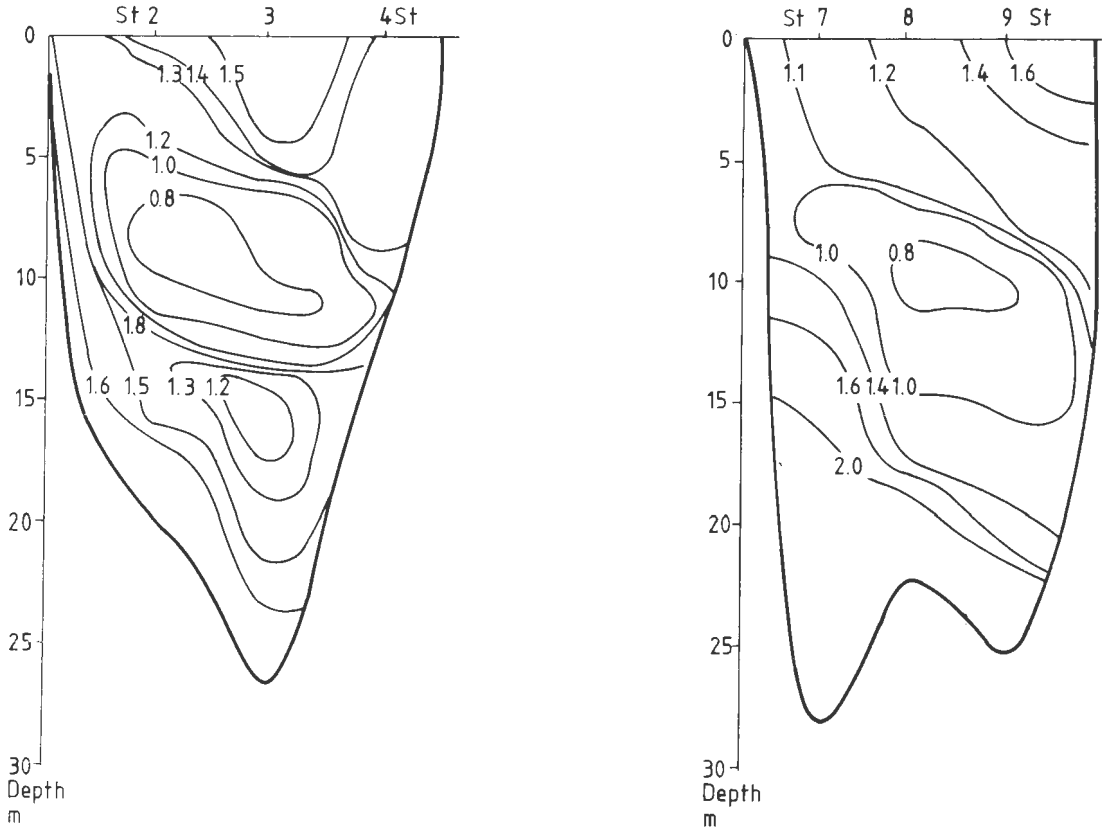

Figure 21. Distribution of c_p, attenuation coefficient due to particles. Transversal section. 781002

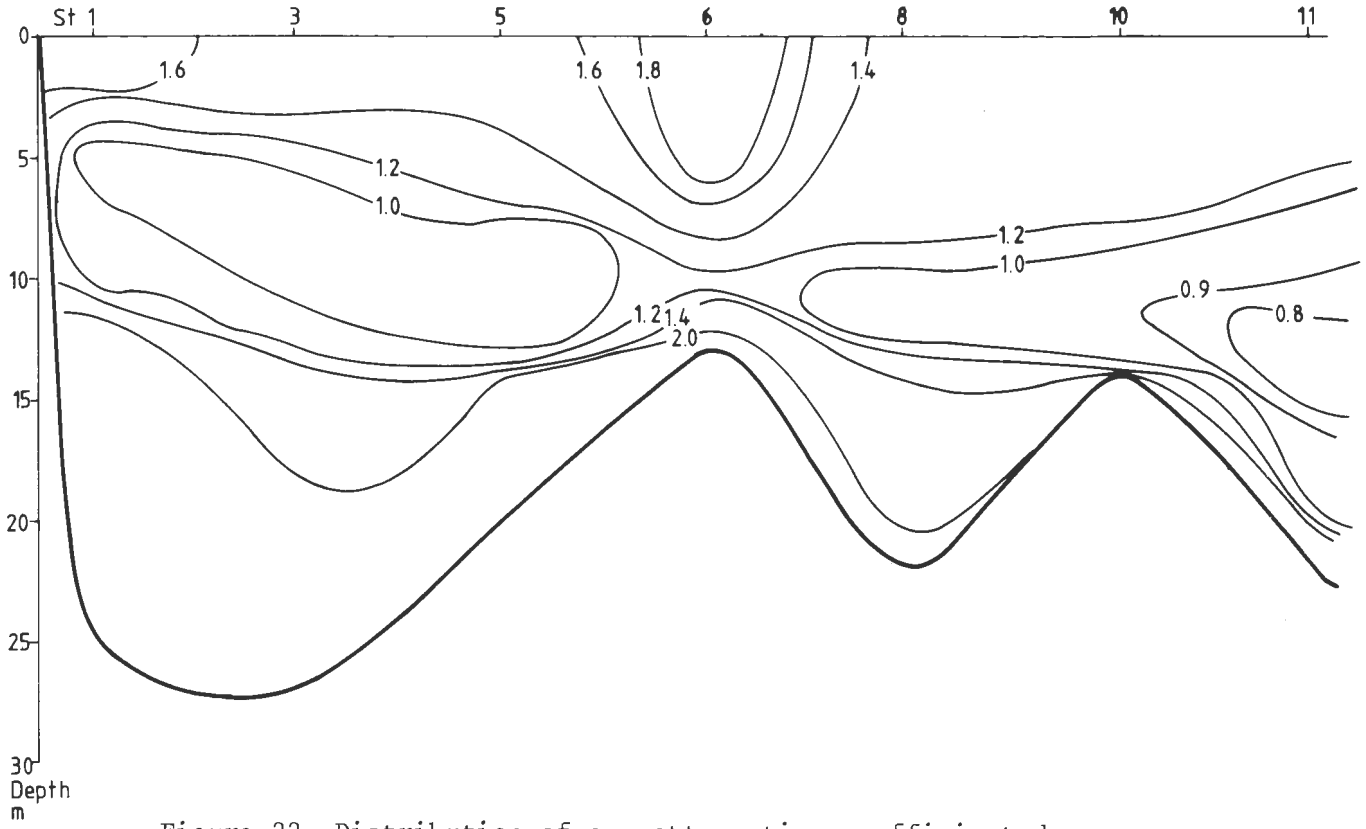

Figure 22. Distribution of c_p, attenuation coefficient due to particles. Longitudinal section. 781005

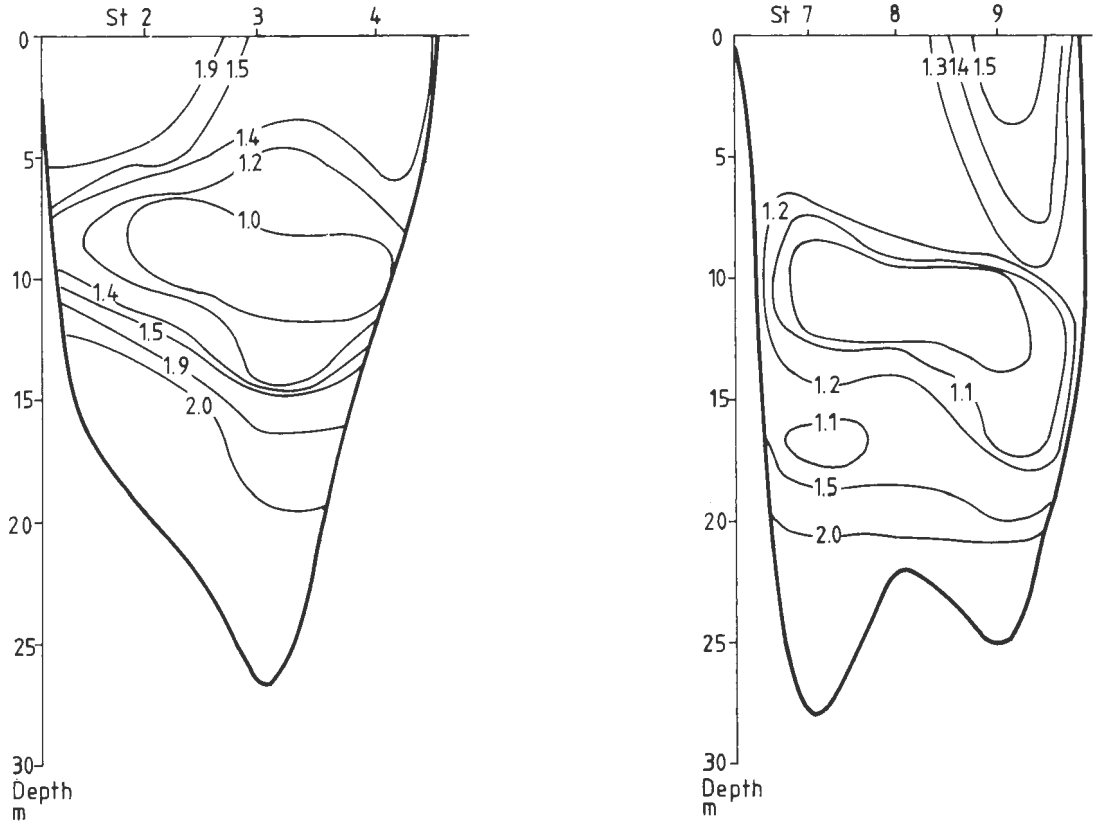

Figure 23. Distribution of c_p, attenuation coefficient due to particles. Transversal section. 781005

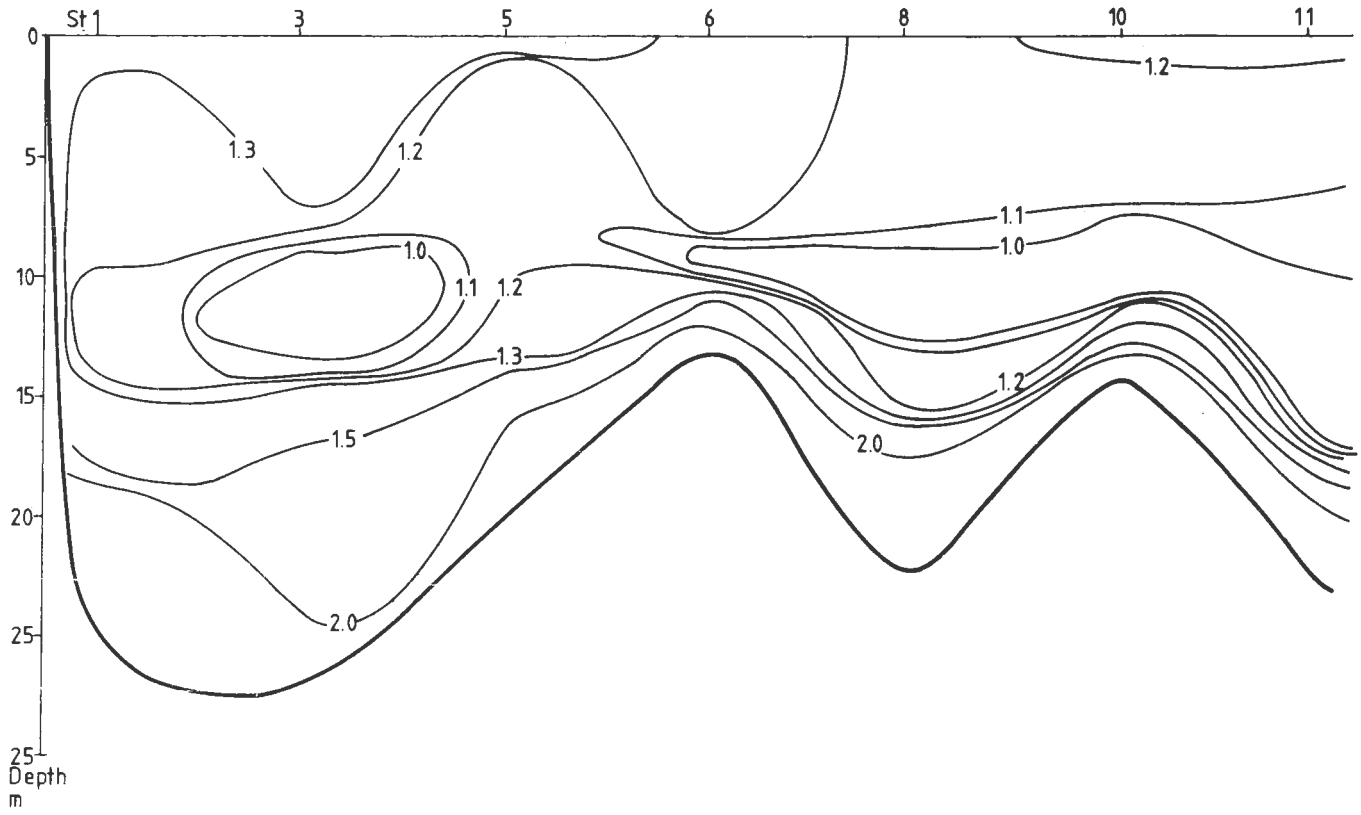

Figure 24. Distribution of c_p, attenuation coefficient due to particles. Longitudinal section. 781006

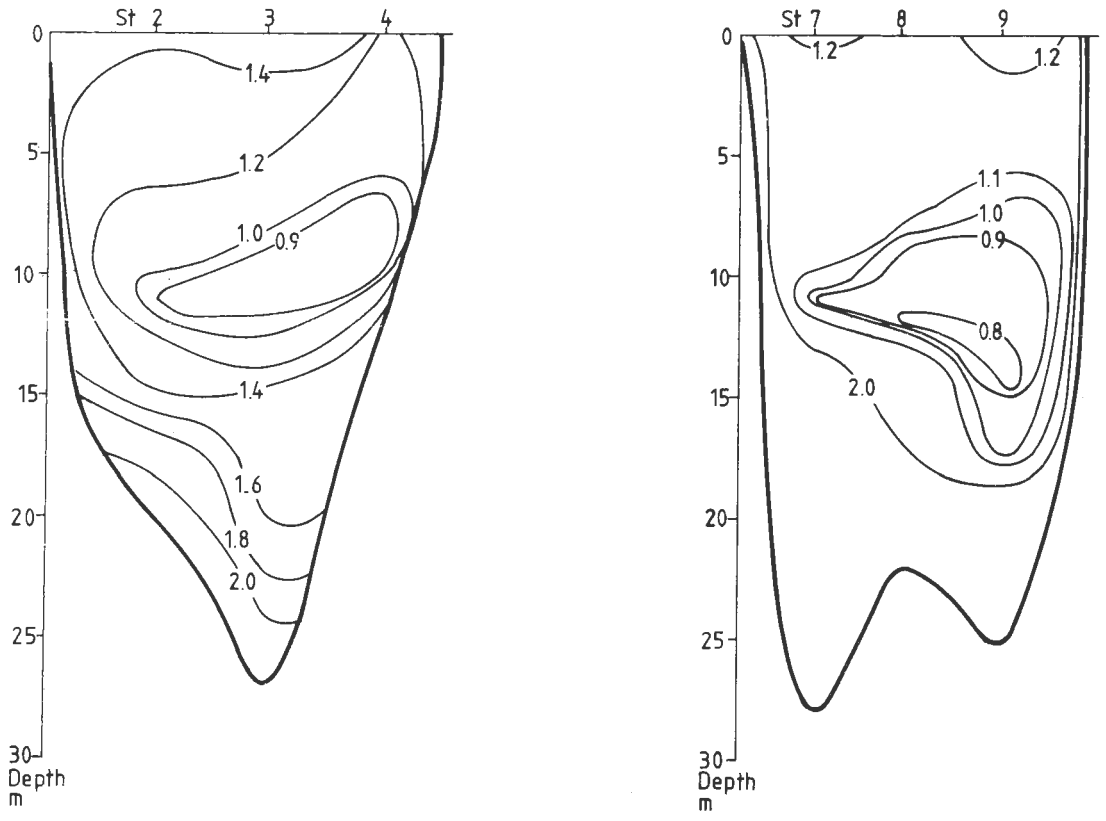

Figure 25. Distribution of c_p, attenuation coefficient due to particles. Transversal section. 781006

SMHI Rapporter

HYDROLOGI OCH OCEANOGRAFI

Nr RHO 1 Weil, J G
Verification of heated water jet numerical model, Stockholm 1974

Nr RHO 2 Svensson, J
Calculation of poison concentrations from a hypothetical accident off the Swedish coast, Stockholm 1974

Nr RHO 3 Vasseur, B
Temperaturförhållanden i svenska kustvatten, Stockholm 1975

Nr RHO 4 Svensson, J
Beräkning av effektiv vattentransport genom Sunninge sund, Stockholm 1975

Nr RHO 5 Bergström, S och Jönsson, S
The application of the HBV runoff model to the Filefjell research basin, Norrköping 1976

Nr RHO 6 Wilmot, W
A numerical model of the effects of reactor cooling water on fjord circulation, Norrköping 1976

Nr RHO 7 Bergström, S
Development and application of a conceptual runoff model, Norrköping 1976

Nr RHO 8 Svensson, J
Seminars at SMHI 1976-03-29--04-01 on numerical models of the spreading of cooling water, Norrköping 1976

Nr RHO 9 Simons, J, Funkquist, L och Svensson, J
Application of a numerical model to Lake Vänern, Norrköping 1977

Nr RHO 10 Svensson, S
A statistical study for automatic calibration of a conceptual runoff model, Norrköping 1977

Nr RHO 11 Bork, I
Model studies of dispersion of pollutants in Lake Vänern, Norrköping 1977

Nr RHO 12 Fremling, S
Sjöisars beroende av väder och vind, snö och vatten, Norrköping 1977

Nr RHO 13 Fremling, S
Sjöisars bärighet vid trafik, Norrköping 1977

Nr RHO 14 Bork, I
Preliminary model studies of sinking plumes, Norrköping 1978

Nr RHO 15 Svensson, J och Wilmot, W
A numerical model of the circulation in Öresund. Evaluation of the effect of a tunnel between Helsingborg and Helsingör, Norrköping 1978

Nr RHO 16 Funkqvist, L
En inledande studie i Vätterns dynamik, Norrköping 1978

Nr RHO 17 Vasseur, B
Modifying a jet model for cooling water outlets, Norrköping 1979

Nr RHO 18 Udin, I och Mattisson, I
Havsis - och snöinformation ur datorbearbetade satellitdata - en metodstudie, Norrköping 1979

Nr RHO 19 Ambjörn, C och Gidhagen, L
Vatten- och materialtransporter mellan Bottniska viken och Östersjön, Norrköping 1979

Nr RHO 20 Gottschalk, L och Jutman, T
Statistical analysis of snow survey data, Norrköping 1979

Nr RHO 21 Eriksson, B
Sveriges vattenbalans. Årsmedelvärde (1931-60) av nederbörd, avdunstning och avrinning

Nr RHO 22 Gottschalk, L and Krasovskaia, I
Synthesis, processing and display of comprehensive hydrologic information

Nr RHO 23 Svensson, J
Sinking cooling water plumes in a numerical model, Norrköping 1980

Nr RHO 24 Vasseur, B, Funkqvist, L och Paul, J F
Verification of a numerical model for thermal plumes, Norrköping 1980

Nr RHO 25 Eggertsson, L-E
HYPOS - ett system för hydrologisk positionsangivelse, Norrköping 1980

Nr RHO 26 Buch, E
Turbulent mixing and particle distribution investigations in the Himmerfjärd 1978
Norrköping 1980

SMHIs tryckeri, Norrköping 1981.

SVERIGES METEOROLOGISKA OCH HYDROLOGISKA INSTITUT
Folkborgsvägen 1, Box 923, 601 19 Norrköping. Telefon 011-108000.